Selective Effect of Guest Molecule Length and Hydrogen Bonding on the Supramolecular Host Structure

Dongxia Wu,[†,§] Ke Deng,[‡] Qingdao Zeng,*[,†] and Chen Wang*[,‡]

Center for Molecular Science, Institute of Chemistry, Chinese Academy of Sciences, Beijing, 100080, P. R. China, National Center for NanoScience and Technology, Beijing, 100080, P. R. China, and Graduate School of Chinese Academy of Sciences, Beijing, 100080, P. R. China

Received: June 19, 2005; In Final Form: August 25, 2005

A host supramolecular structure consisting of bis-(2,2′:6′,2″-terpyridine)-4′-oxyhexadecane (BT−O−C16) is shown to respond to guest molecules in dramatic ways, as observed by using scanning tunneling microscopy (STM) on a highly oriented pyrolytic graphite surface under ambient conditions. It is observed that small linear molecules can be encapsulated within the host supramolecular lattice. The characteristics of the host structure were nearly unaffected by the encapsulated guest molecules of terphthalic acid (TPA) dimers, whereas appreciable changes in cavity dimension can be observed with azobenzene-4,4′-dicarboxylic acid. The STM study and density functional theory (DFT) analysis reveal that intermolecular hydrogen bonding interaction plays an essential role in forming the assembling structures. The difference in guest molecule length is considered the important cause for the different guest−host complexes.

Introduction

The weak intermolecular interactions, such as van der Waals force and hydrogen bonding, between guest and host species are well known to affect the host structures. Such interactions may cause distortions in lattice geometries.[1−3] Such flexibility in host frameworks has been very important for molecular recognitions such as in drug−receptor complexes.[4] The extent of the impact on the host structures range from conformational variation to dramatic alternation of the host structures, or polymorphism effect.

There are a number of reports on the direct observation of guest inclusion effects using two-dimensional (2D) molecular lattices as the host structure. For example, a hydrogen bonded molecular network formed by perylene tetracarboxylic diimide (PTCDI) and 1,3,5-triazine-2,4,6-triamine (melamine) was obtained on a Ag/Si(111)-($\sqrt{3} \times \sqrt{3}$)R30° surface under ultrahigh vacuum (UHV) conditions.[5] Such a supramolecular network adopts a hexagonal pattern with a lattice constant of 34.6 Å. The open pores can be packed in with up to seven C_{60} molecules. The adsorption registry of C_{60} heptomers is clearly resolved and differs from that of C_{60} on Ag/Si(111)-($\sqrt{3} \times \sqrt{3}$)-R30°. This is a reflection of the confinement effect due to the host lattice structure. In addition, the C_{60} can also adsorb directly on top of the PTCDI and melamine molecules, leading to a replicated lattice structure.

Recent studies showed that coronene (COR) and C_{60} molecules can also be immobilized within hexagonal organic networks of 1,3,5-benzenetricarboxylic acid (trimesic acid, TMA).[6−8] For the $(TMA)_2$·COR complex, it was suggested that the entrapped guest COR molecules were stabilized by hydrogen bonds to the host network.[8] The conclusion was drawn from X-ray diffractometer measurements of the $(TMA)_2$·HEL complex, in which COR is replaced by the structurally similar molecule of hexahelicene (HEL). One may note that the $(TMA)_2$·COR complex could be prepared by different methods, that is, coadsorption on a graphite surface and cocrystallization. Considering that the graphite surface interacts with the TMA and COR adsorbates through nonspecific interaction (van der Waals interaction), the nature of the intermolecular interaction for surface-assembled $(TMA)_2$·COR complex should be the same as those encountered for cocrystals.

In a separate study, the molecular inclusion of molecules of phthalocyanine and COR within the tetragonal network of 1,3,5-tris(10-carboxydecyloxy)benzene (TCDB) leads to an appreciable expansion or contraction of the host cavities, reflecting different degrees of guest−host interactions.[9]

By utilizing the various geometries and functionalities of the building units, a broad range of host structures can be obtained that provide us with a rich ground for explorations. To control the ordering of molecules in the 2D monolayer structure, directional interactions of hydrogen bonds are of great importance.[10−17]

Terpyridine molecules are well known for their ability to form stable complexes with a variety of transition metal ions.[18] Today, they represent one of the most interesting ligands in the fields of metallosupramolecular chemistry because of their special electrochemical and photochemical properties. Many groups have reported research on the terpyridine molecules, using them as building blocks in metallosupramolecular engineering. Very recently, several examples for preparing a new class of nanomaterials based on terpyridines have been reported.[19−23]

In this work, we report the construction of a supramolecular structure using a terpyridine derivative. The lamella-type host structure is expected to accommodate short linear molecules. The guest species were introduced through a coadsorption approach and were observed by using scanning tunneling microscopy (STM) under ambient conditions. It was identified that the inclusion of the guest species is highly selective for

* Corresponding authors. E-mail: stmzqd@iccas.ac.cn (Q.Z.); wangch@iccas.ac.cn (C.W.).
† Chinese Academy of Sciences.
‡ National Center for NanoScience and Technology.
§ Graduate School of Chinese Academy of Sciences.

10.1021/jp053293x CCC: $30.25
Published on Web 11/09/2005

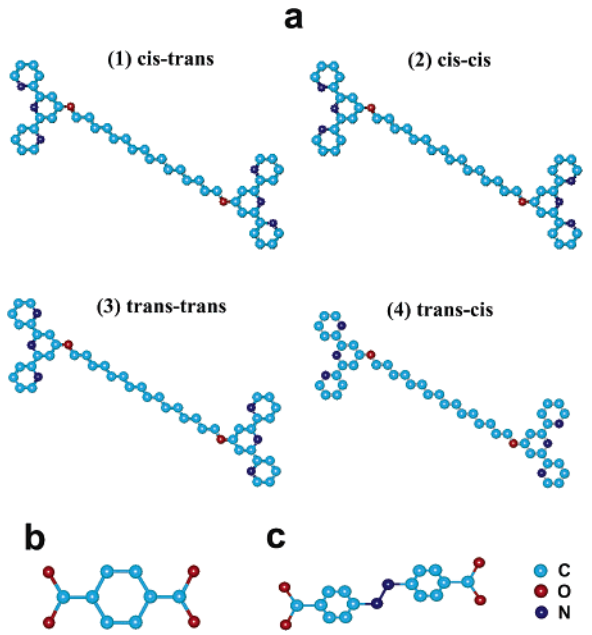

Figure 1. Molecular structures of (a) BT−O−C16: (1) cis−trans, (2) cis−cis, (3) trans−trans, (4) trans−cis); (b) TPA; and (c) azobenzene-4,4′-dicarboxyl acid.

SCHEME 1: Synthesis of the BT−O−C16 Molecule.

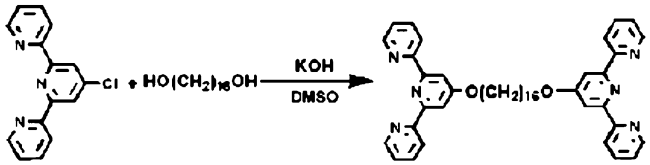

hydrogen bonds and molecular length; that is, only molecules with an appropriate length and terminal hydrogen bonds can be immobilized under ambient conditions. The host and guest molecules studied here are shown in Figure 1. Combining our observations with theoretical analysis, we concluded that both of the guest molecules of terphthalic acid (TPA) (in the form of dimers) and azobenzene-4,4′-dicarboxylic acid are connected to the host lattice via an O−H···N hydrogen bond with comparable bond length. Furthermore, it was observed that the guest species can induce varied conformational changes in the host lattice, which are manifested as altered cavity dimensions. The cause for the varied host structure can be associated with the appreciable length difference between TPA dimers and azobenzene-4,4′-dicarboxylic acid. TPA dimers can fit into the host cavity without requiring much adjustment, and the cavity geometry remains nearly intact. In contrast, the azobenzene-4,4′-dicarboxylic acid, having less length, leads to significant distortion of the host cavity. This study demonstrates that the STM method could provide useful insight into the flexibility of 2D host structures under the influence of guest molecule geometry.

Experimental and Computational Details

The synthetic route to the designated molecules of bis-(2,2′:6′,2″-terpyridine)-4′-oxyhexadecane (BT−O−C16) is shown in Scheme 1. All of the chemicals used were purchased from Acros and Fluka and used without further purification.

The BT−O−C16 molecules were synthesized as follows:[21] Hexadecane-1,16-diol (897 mg, 3.47 mmol) was slowly added to a stirred suspension of powdered KOH (1.87 g, 33.4 mmol) in dry dimethyl sulfoxide (DMSO; 30 mL) at 80 °C. After 30 min, 4′-chloro-2,2′:6′,2″-terpyridine was added (1.86 g, 6.94 mmol), and the mixture was stirred for 12 h at 70 °C and then poured into 200 mL of distilled water. The aqueous phase was extracted with CH_2Cl_2 (5 × 100 mL). The combined organic phases were evaporated under ambient conditions. The residue was recrystallized from ethyl acetate. The details of the characterization of this compound can be found in the Supporting Information.

The solvent used in the STM experiments was toluene (HPLC grade, Aldrich). The guest molecules used in this study were TPA and azobenzene-4,4′-dicarboxylic acid, as shown in Figure 1. TPA and azobenzene-4,4′-dicarboxylic acid were obtained from TCI and used without further purification. The concentration of all the solutions used was less than 1 mM. The samples were prepared by depositing a drop of the solution containing the compound on a freshly cleaved, atomically flat surface of highly oriented pyrolytic graphite (HOPG). After the solvent was evaporated, the experiments were performed with a Nanoscope IIIA system (Digital Instrument, Santa Barbara, CA) operating under ambient conditions. The STM tips were mechanically formed Pt/Ir wire (80/20). All of the STM images were recorded using the constant current mode. The specific tunneling conditions are given in the figure captions.

We perform the theoretical calculation using the density functional theory (DFT) provided by the DMol3 code.[24] The Perdew and Wang parametrization[25] of the local exchange-correlation energy is applied in the local spin density approximation (LSDA) to describe the exchange and correlation. We expand the all-electron spin-unrestricted Kohn−Sham wave functions in a local atomic orbital basis. In the double-numerical basis set, the valence *s* and *p* orbitals are represented by two basis functions each, and the *d* type wave function on each atom has been used to describe polarization. An angular momentum number, one greater than the maximum angular momentum number in the atomic orbital basis, is applied to specify the multipolar fitting that describes the analytical forms of the charge density and the Coulombic potential. All calculations are all-electron ones and are performed with extra-fine mesh. Self-consistent field procedure is done with a convergence criterion of 10^{-5} a.u. on the energy and electron density.

Results and Discussions

1. Self-Assembly of BT−O−C16. A large-scale image of a well-ordered BT−O−C16 arrangement is exhibited in Figure 2a. BT−O−C16 formed a close-packed ladder-like structure. The bright spots are attributed to the terpyridine cores of BT−O−C16, while the chains attached to the spots represent the long alkyl chains between the terpyridine cores. The length of the alkyl chain is measured to be about 2.1 ± 0.1 nm, which is consistent with the calculated length of hexadecane. The headgroup terpyridines from neighboring BT−O−C16 molecules are aligned in long uniform double rows. One may notice that, in Figure 2a, it is discernible that adjacent pyridine groups form a dimer-like structure. The host network structure is characterized by the rhombus cavities, which are about 1.0 ± 0.1 nm wide along the *a* direction and 2.1 ± 0.1 nm long along the *b* direction (shown in Figure 2a), and the angle between headgroup rows and the alkyl lamella direction is about 93 ± 2°. We present the theoretically simulated molecular packing model by the DFT method in Figure 2b on the basis of STM observation, in which the BT−O−C16 molecule displays cis−trans conformation. Since pyridine groups can rotate with little torsion energy, a single BT−O−C16 molecule could have several conformational isomers. We have theoretically tested

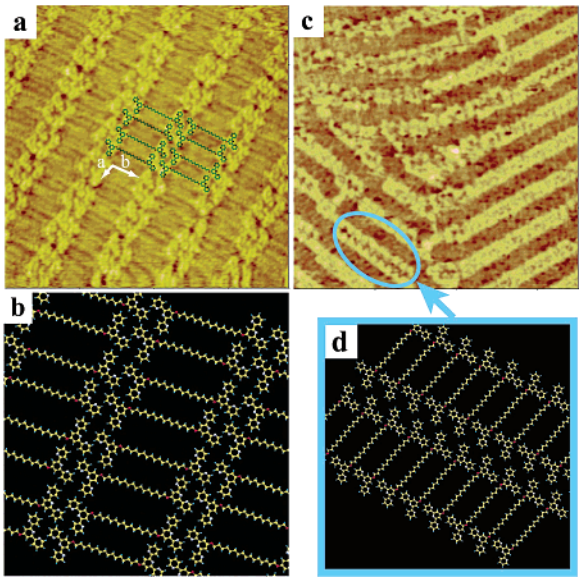

Figure 2. (a) STM image (19 × 19 nm) of a self-assembled monolayer of BT−O−C16 on HOPG. The tunneling conditions are $I = 580$ pA and $V = 750$ mV. (b) Molecular model for the 2D packing of BT−O−C16 molecules. (c) STM image (35 × 35 nm) of a self-assembled monolayer of BT−O−C16 showing the coexistence of lamellae with two different separations between the terpyridine headgroups. The tunneling conditions are $I = 600$ pA and $V = 650$ mV. (d) Proposed molecular model with trans−trans terpyridine headgroups for BT−O−C16.

all of the isomers, namely, cis−trans, cis−cis, trans−trans, and trans−cis (shown in Figure 1a), and found that all of them could construct the ladder-like network; however, the cis−trans BT−O−C16 and cis−cis BT−O−C16 are the preferential conformations. It is clearly noted that all of the conformation isomers could form a C−H···O hydrogen bond between the oxygen atom in the alkyl chain and the hydrogen atom of the pyridine group in a alkyl-chain-parallel neighboring molecule. The simulation results reveal that cis−trans or cis−cis BT−O−C16 isomers could form the C−H···N hydrogen bond between the head-to-head neighbors. Our theoretical calculations show that the lengths of the C−H···O hydrogen bonds in the assembly constructed by the four different conformation isomers are nearly equal (∼3.26 Å), and the binding energy of the side-by-side dimer interaction is ∼8.0 kcal mol^{-1}. For the head-to-head interaction, because the C−H···N hydrogen bond is formed, the binding energies for the assembly of the cis−trans and cis−cis BT−O−C16 isomers are 9.0 and 12.0 kcal mol^{-1}, respectively. These data are in agreement with the typical characteristic of hydrogen bonds. We also found that because of the absence of strong intermolecular interactions (hydrogen bonding) between the head-to-head neighbors, the binding energies for the assembly of the trans−trans and trans−cis isomers are about 1.7 and 3.0 kcal mol^{-1}, respectively.

In Figure 2c, an STM image is presented showing the coexistence of lamellae with two different separations between the terpyridine headgroups. A proposed molecular model is shown in Figure 2d, illustrating the trans−trans terpyridine headgroups for BT−O−C16. The difference in clearance width between the BT−O−C16 headgroups is attributed to the different molecular conformational isomers, including cis−cis, cis−trans, trans−trans, and trans−cis. Specifically, we consider that the wider clearance is associated with the trans−trans or trans−cis conformation of BT−O−C16 headgroups (illustrated

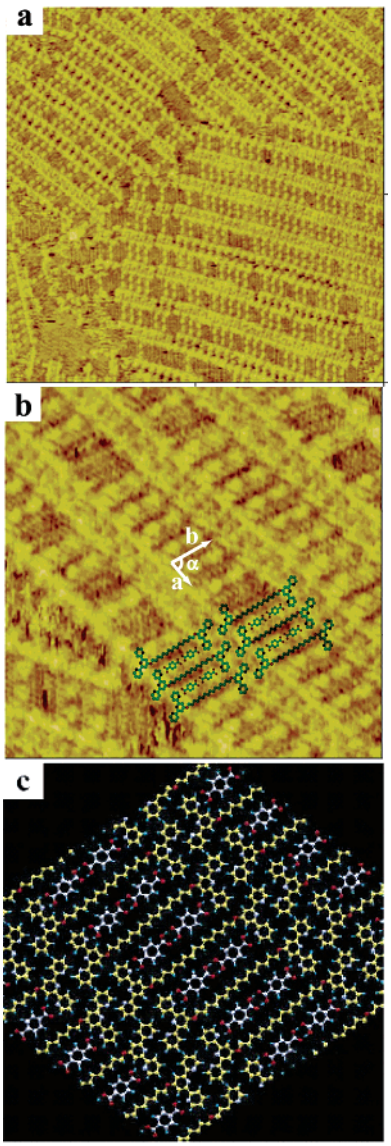

Figure 3. (a) STM image (50 × 50 nm) of a self-assembled monolayer of TPA/BT−O−C16 on HOPG. The tunneling conditions are $I = 600$ pA and $V = 600$ mV. (b) High-resolution STM image (15 × 15 nm) of TPA/BT−O−C16 coadsorbed on HOPG. The tunneling conditions are $I = 600$ pA and $V = 600$ mV. (c) Molecular model representing the assembly structure of the TPA/BT−O−C16 complex.

in Figure 1a) because of the absence of strong intermolecular interactions (hydrogen bonding) between the BT−O−C16 headgroups.

2. Inclusion Effect of Linear Guest Species with Terminal Hydrogen Bonds. The inclusion properties of BT−O−C16 host networks can be readily observed by adding a small linear molecule such as TPA and azobenzene-4,4′-dicarboxyl acid. The lamella characteristics of the host lattice geometry persist as in the homogeneous assembly of BT−O−C16, and the TPA guest molecules are positioned in the cavities of the alkane ladders. However, because of the difference in the molecular lengths, the impact of TPA and azobenzene-4,4′-dicarboxyl acid on the host BT−O−C16 lattice is different, as presented below.

Upon the introduction of TPA as the coadsorption agent, the structure of the TPA/BT−O−C16 complex reveals that the TPA molecules, as the guest molecule, are entrapped in the cavities between the alkyl chains of BT−O−C16 (see Figure 3a). The adsorbed TPA dimers are stable under STM observations without any evidence of migration. It can also be noted in this

figure that both wide and narrow separations between the terpyridine headgroups coexist. Since these types of headgroup separations are also observed in the assembly structure of BT−O−C16 itself, as shown in Figure 2c, it does not necessarily represent an effect of the guest molecule inclusion.

The more detailed adsorption structure of TPA entrapped in the BT−O−C16 lamella is shown in Figure 3b. The small bright spots in the BT−O−C16 lamellae are ascribed to the aromatic rings of TPA. Two small bright spots can be clearly recognized in the cavities of the BT−O−C16 ladders, with the measured distance of about 1.0 ± 0.1 nm between the centers of the two spots. The observed dimer structure is considered to be TPA molecules connected via hydrogen bonds between the carboxyl groups. This is also confirmed by our DFT calculations, in which the TPA forms dimers by strong hydrogen bonds between the end carboxyl groups, with an O−H···O distance of ∼2.4 Å, and the distance of the dimer's aromatic ring centers is ∼9.4 Å. The measured dimensions of the TPA-inserted cavity (length, width, and the angle between the alkyl chain and the terpyridine rings of BT−O−C16) were almost the same as those of the original unfilled network of BT−O−C16. By comparing the measured cavity length (∼2.1 nm) and the calculated length of the TPA dimer (∼1.8 nm), we conclude that the TPA dimer can ideally fit into the cavity and form hydrogen bonds with the terpyridines (between the end carboxyl group of the TPA dimer and the N atom in the pyridine group of the BT−O−C16) without requiring significant structural adjustments. This could serve as an example of the well-known rigid lock-and-key model.[26]

According to the image shown in Figure 3b, a theoretical molecular model to illustrate the assembly structure is given, and the most probable BT−O−C16 molecules in the network would be the cis−trans conformation. Theoretical study shows that the guest TPA dimers strongly interact with the host BT−O−C16 framework by forming O−H···N hydrogen bonds between the end carboxyl group of TPA and the N atom in the terpyridine headgroup of BT−O−C16, in which the distance of the O−H···N hydrogen bond is ∼2.6 Å, and the H···N distance is ∼1.4 Å. The binding energy for each TPA dimer is ∼59.5 kcal mol^{-1}. Such interaction is so strong that its strength could be compared with that of covalent bonding.

Azobenzene-4,4′-dicarboxyl acid molecules in the cavities are sufficiently stable to endure repeated scanning, and the ordered assembly could be observed as shown in Figure 4a. In Figure 4a, only one brighter clubbed part is identified in the cavity of the network of BT−O−C16, which is ascribed to the N═N bridged benzene cores of the azobenzene-4,4′-dicarboxyl acid molecule. The high-resolution image in Figure 4b reveals more details. The length of the azobenzene-4,4′-dicarboxyl acid-filled cavity is 1.9 ± 0.1 nm, and the width is 1.2 ± 0.1 nm. In addition, the angle between the alkyl chain and the terpyridine rings of BT−O−C16 is increased to 124 ± 2°. Obviously, the changes in the cavity dimensions correspond to the difference in molecular length between the TPA and azobenzene-4,4′-dicarboxyl acid molecules. Here, we consider that the azobenzene-4,4′-dicarboxyl acid molecule in the assembly is the trans form, because the trans form is the stable conformation under ambient conditions. The trans-form azobenzene-4,4′-dicarboxyl acid molecule is expected to have characteristics as a qualitatively straight rod structure, which is consistent with the observed characteristics in Figure 4a,b. In the trans form, the calculated length of azobenzene-4,4′-dicarboxyl acid is ∼1.5 nm, which is 0.3 nm shorter than that of one TPA dimer, which is appreciably less than the length of the unfilled cavity of BT−O−C16 (∼2.1 nm). A theoretical molecular model to illustrate the assembly structure is given in Figure 4c. Theoretical study shows that the guest azobenzene-4,4′-dicarboxyl acid molecule strongly interacts with the host BT−O−C16 framework by forming the O−H···N hydrogen bond through the end carboxyl group of azobenzene-4,4′-dicarboxyl acid and the N atom in the terpyridine headgroup of BT−O−C16, in which the distance of the O−H···N hydrogen bond is ∼2.8 Å (the H···N distance is ∼1.85 Å) and the binding energy of the interaction is ∼31.3 kcal mol^{-1}. As a result of such strong hydrogen bonding and the mismatch of the lengths of the guest molecule and the host cavity, the original O−H···O hydrogen bond between the side-by-side BT−O−C16 molecules is broken. However, the lamella network is still stable because the inserted azobenzene-4,4′-dicarboxyl acid molecule forms a strong O−H···N hydrogen bond with the BT−O−C16 molecules. The observed evidence of the guest-induced cooperative structural variation of the host lattice could be considered an example of a mutually induced

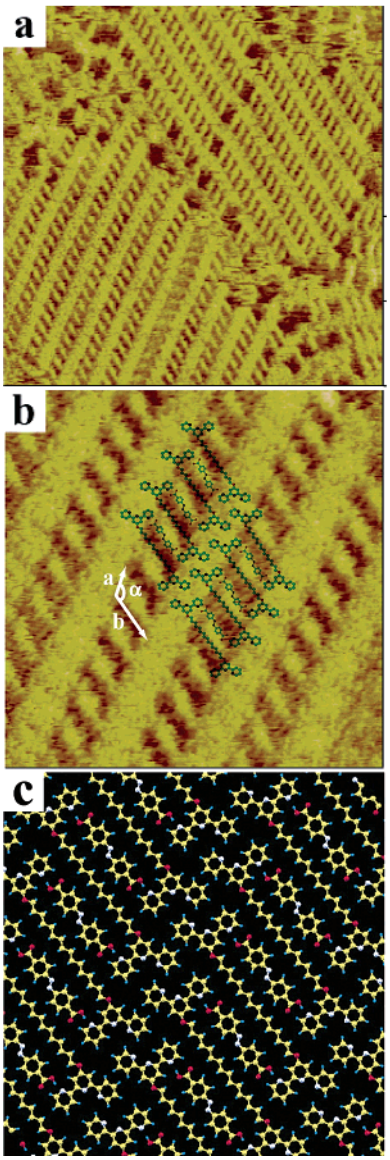

Figure 4. (a) STM image (45 × 45 nm) of a self-assembled monolayer of azobenzene-4,4′-dicarboxyl acid/BT−O−C16 on HOPG. (b) High-resolution STM image (14 × 14 nm) of azobenzene-4,4′-dicarboxyl acid/BT−O−C16 coadsorbed on HOPG. The tunneling conditions are I = 600 pA and V = 620 mV. (c) Molecular model representing the assembly structure of the azobenzene-4,4′-dicarboxyl acid/BT−O−C16 complex.

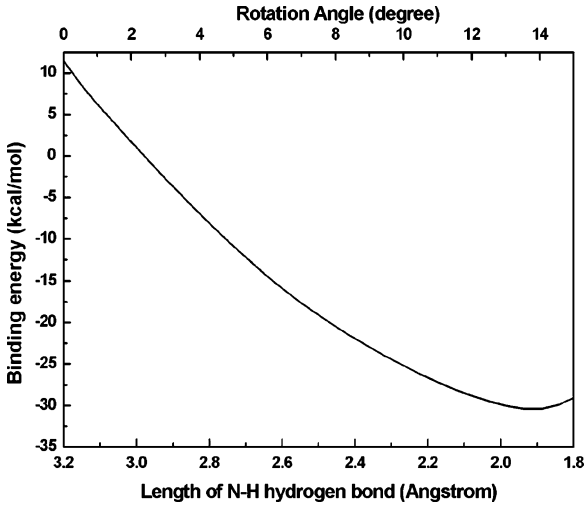

Figure 5. Theoretical simulations to investigate the distortion of the BT−O−C16 framework during the azobenzene-4,4′-dicarboxyl acid insertion into the cavity. The binding energy equals the total energy of the complex system minus the energy of the unfilled BT−O−C16 system and the separate guest molecule. The positive binding energy means the system is unstable, whereas the negative binding energy means the system is stable. The BT−O−C16 framework distorts gradually with the rotation angle changing from 0 to 15°, and the length of H···N hydrogen bond shortens gradually from 3.2 to 1.8 Å.

fit mechanism,[27] in which both the guest and the host structures are optimized to achieve stabilized complex.

We performed theoretical simulations to investigate the dynamic process of this distortion of the BT−O−C16 framework during the azobenzene-4,4′-dicarboxyl acid insertion into the cavity. The energy dependence on H···N length is presented in Figure 5. It shows that, at first, when an azobenzene-4,4′-dicarboxyl acid molecule is inserted in the center of the undistorted cavity, the binding energy of the system is positive, which means the system is unstable. During the subsequent process, the BT−O−C16 molecule rotates gradually, and the length of the O−H···N hydrogen bond between the azobenzene-4,4′-dicarboxyl acid and BT−O−C16 is also gradually reduced. When such distortion of the BT−O−C16 framework is completed, the binding energy of the system changes from positive to negative; that is, the system becomes more stable compared to the starting structure. In Figure 5, we can see that the system would be the most stable when the rotation angle of the cavity is about 14° and length of the H···N hydrogen bond is about 1.9 Å. As a result of such host lattice distortion, the calculated angle between the alkyl chain and the terpyridine rings of BT−O−C16 is increased to about 124°, which agrees with the measured value.

Theoretical analysis leads to the conclusion that the carboxyl groups are connected to the terpyridine headgroups via hydrogen bonds, which is a crucial factor stabilizing the coadsorption structure. We also studied the inclusion effect of several other linear molecules (such as 1,4-bis[β-pyridyl-(2)-vinyl]benzene (P2VB) and pentacene) that are similar in length to TPA dimers and azobenzene-4,4′-dicarboxylic acid but without the carboxyl terminal groups. The inclusion evidence can only rarely be observed for those molecules. This observation confirms that the hydrogen bond of the guest molecules to the terpyridine headgroups is an critical factor for stabilizing guest species.

Furthermore, we attempted a coadsorption experiment using benzoic acid as the guest. We could only obtain the linear array lamella structure of the host, and no benzoic acid molecules could be observed in the cavities between the alkyl chains of BT−O−C16. The result could be attributed to the absence of hydrogen bonding between BT−O−C16 and benzoic acid. Therefore, it can be concluded that the incorporation of intermolecular hydrogen bonding is a vital factor that stabilizes the coadsorption structure in this host−guest system, in addition to the size matching requirements.

Conclusion

The guest−host interaction can lead to appreciable variation to the interactions between the building units of the host lattice. This study provides an example in which the geometry of the host cavity could be self-adjusted to accommodate the guest molecules. Such host structure flexibility is achieved through adjusting the bonding of the host supramolecular structures. The results also demonstrate that STM can be an effective approach for studying geometrical effects on 2D guest−host architectures.

Acknowledgment. Financial support from the National Natural Science Foundation of China (Grant Nos. 20473094, 20573116, 90406019, and 90406024) and Chinese Academy of Sciences is gratefully acknowledged. The authors also wish to thank Prof. Chunli Bai for many constructive discussions and Dr. Yanlian Yang for assistance in preparing the manuscript.

Supporting Information Available: Synthesis details of BT−O−C16. This material is available free of charge via the Internet at http://pubs.acs.org.

References and Notes

(1) Thaimattam, R.; Xue, F.; Sarma, J. A. R. P.; Mak, T. C. W.; Desiraju, G. R. *J. Am. Chem. Soc.* **2001**, *123*, 4432.
(2) Matsuda, R.; Kitaura, R.; Kitagawa, S.; Kubota, Y.; Kobayashi, T. C.; Horike, S.; Takata, M. *J. Am. Chem. Soc.* **2004**, *126*, 14063.
(3) Grave, C.; Lentz, D.; Schafer, A.; Samori, P.; Rabe, J. P.; Franke, P.; Schluter, A. D. *J. Am. Chem. Soc.* **2003**, *125*, 6907.
(4) Davis, A. M.; Teague, S. J. *Angew. Chem., Int. Ed.* **1999**, *38*, 736.
(5) Theobald, J. A.; Oxtoby, N. S.; Phillips, M. A.; Champness, N. R.; Beton, P. H. *Nature* **2003**, *424*, 1029.
(6) Griessl, S. J. H.; Lackinger, M.; Jamitzky, F.; Markert, T.; Hietschold, M.; Heckl, W. M. *Langmuir* **2004**, *20*, 9403.
(7) Griessl, S. J. H.; Lackinger, M.; Jamitzky, F.; Markert, T.; Hietschold, M.; Heckl, W. M. *J. Phys. Chem. B* **2004**, *108*, 11556.
(8) Ermer, O.; Neudörfl, J. *Helv. Chim. Acta* **2001**, *84*, 1268.
(9) Lu, J.; Lei, S. B.; Zeng, Q. D.; Kang, S. Z.; Wang, C.; Wan, L. J.; Bai, C. L. *J. Phys. Chem. B* **2004**, *108*, 5161.
(10) Feyter, S. D.; Gesquiere, A.; Abdel-Mottaleb, M. M.; Grim, P. C. M.; Schryver, F. C. D.; Meiners, C.; Sieffert, M.; Valiyaveettil, S.; Mullen, K. *Acc. Chem. Res.* **2000**, *33*, 520.
(11) Dmitriev, A.; Spillmann, H.; Lin, N.; Barth, J. V.; Kern, K. *Angew. Chem., Int. Ed.* **2003**, *42*, 2670.
(12) Yokoyama, T.; Yokoyama, S.; Kamikado, T.; Okuno, Y.; Mashiko, S. *Nature* **2001**, *413*, 619.
(13) Gottarelli, G.; Masiero, S.; Mezzina, E.; Pieraccini, S.; Rabe, J. P.; Samori, P.; Spada, G. P. *Chem.—Eur. J.* **2000**, *6*, 3242.
(14) Lei, S. B.; Wang, C.; Yin, S. X.; Wang, H. N.; Xi, F.; Liu, H. W.; Xu, B.; Wan, L. J.; Bai, C. L. *J. Phys. Chem. B* **2001**, *105*, 10841.
(15) Feyter, S. D.; Schryver, F. C. D. *J. Phys. Chem. B* **2005**, *109*, 4290.
(16) Gyarfas, B. J.; Wiggins, B.; Zosel, M.; Hipps, K. W. *Langmuir* **2005**, *21*, 919.
(17) Lackinger, M.; Griessl, S.; Heckl, W. M.; Hietschold, M.; Flynn, G. W. *Langmuir* **2005**, *21*, 4984.
(18) Thompson, A. M. W. C. *Coord. Chem. Rev.* **1997**, *160*, 1.
(19) Schubert, U. S.; Eschbaumer, C. *Angew. Chem.* **2002**, *114*, 3016; *Angew. Chem., Int. Ed.* **2002**, *41*, 2982.
(20) Lohmeijer, B. G. G.; Schubert, U. S. *Angew. Chem.* **2002**, *114*, 3980; *Angew. Chem., Int. Ed.* **2002**, *41*, 3825.
(21) Schubert, U. S.; Eschbaumer, C.; Hien, O.; Andres, P. R. *Tetrahedron Lett.* **2001**, *42*, 4705.
(22) Diaz, J. D.; Bernhard, S.; Storrier, G. D.; Abruna, H. D. *J. Phys. Chem. B* **2001**, *105*, 8746.
(23) Park, J.; Pasupathy, A. N.; Goldsmith, J. I.; Chang, C.; Yaish, Y.; Petta, J. R.; Rinkoski, M.; Sethna, J. P.; Abruna, H. D.; McEuen, P. L.; Ralph, D. C. *Nature* **2002**, *417*, 722.
(24) Becke, A. *J. Chem. Phys.* **1988**, *88*, 2547.
(25) Perdew, J. P.; Wang, Y. *Phys. Rev. B* **1992**, *45*, 13244.
(26) Fischer, E. *Ber. Dtsch. Chem. Ges.* **1894**, *27*, 2985.
(27) Koshland, D. E. *Proc. Natl. Acad. Sci. U.S.A.* **1958**, *44*, 98.